Computational Strategies for Entropy Modeling in Chemical Processes

Wook Shin[1] and Zhongyue J. Yang[1-5,]*

[1]Department of Chemistry, Vanderbilt University, Nashville, Tennessee 37235, United States [2]Center for Structural Biology, Vanderbilt University, Nashville, Tennessee 37235, United States [3]Vanderbilt Institute of Chemical Biology, Vanderbilt University, Nashville, Tennessee 37235, United States [4]Department of Chemical and Biomolecular Engineering, Vanderbilt University, Nashville, Tennessee 37235, United States [5]Data Science Institute, Vanderbilt University, Nashville, Tennessee 37235, United States

Corresponding Author

*Email: zhongyue.yang@vanderbilt.edu Phone: 615-343-9849

ABSTRACT. Computational simulations of entropy are important in understanding the thermodynamic forces that drive chemical reactions on a molecular scale. In recent years, various algorithms have been developed and applied in conjunction with molecular modeling techniques to evaluate the change of entropy in solvation, hydrophobic interactions, and chemical reactions. The aim of this review is to highlight four specific computational entropy calculation methods: normal mode analysis, free volume model, two-phase thermodynamics, and configurational

entropy modeling. The technical aspects, applications, and limitations of each method will be discussed in detail.

KEYWORDS. Entropy calculation, molecular modeling, reaction mechanism, entropy calculation

1. Introduction

Entropic variation accompanies chemical processes, which broadly encompass organic reactions, supramolecular complexation, protein-ligand or protein-protein interactions, alloy formation, catalysis, solvation, and so on. At the molecular level, changes in configurational space during these reactions or interactions lead to an entropy variation. For instance, in the Diels–Alder reaction between 1,3-butadiene and ethylene to form cyclohexene, the removal of 3 translational and 3 rotational degrees of freedom in the process of product formation leads to an entropy reduction. In complex systems, such as those found in solvents or enzymes, the participation of solvent molecules or conformational changes of proteins can complicate chemical reactions or molecular interactions. In these cases, changes in entropy have been observed to balance out changes in enthalpy, playing a role in the enthalpy-entropy compensation effect.[1, 2]

Experimental methods to determine entropic change in chemical reactions and molecular interactions have been established. One way is to calculate entropy using van't Hoff equation by fitting the logarithm of equilibrium constants to the reciprocal of temperature.[3, 4] Other methods include isothermal titration calorimetry[5] and differential scanning calorimetry[6], which measure enthalpy and free energy to determine entropy. Although entropy can be estimated experimentally, the molecular details behind the entropic change are not fully understood.

Computational modeling approaches, including molecular dynamics (MD) and Monte Carlo (MC) simulations, have been developed to investigate the evolution of microscopic states in chemical processes under certain physical conditions (e.g., temperature, pressure, chemical potential, etc.). However, quantification of entropy from molecular ensembles is challenging due to the demand of searching all accessible configurations to calculate the configurational probability density function or partition function. This issue is particularly severe for reactions involving a net change of molecular molar numbers (e.g., bimolecular reactions). Computational strategies have been extensively developed to account for entropic variation of chemical transformations, including Hessian-based methods,[7, 8] direct binning approach,[9] and thermodynamic integration.[10] Methods have also been developed to calculate entropy associated with solvation,[11-14] hydrophobic interaction,[15, 16] and interfacial tension.[17]

Considering the extensive development of theoretical and computational methods for entropy calculation, this review does not intend to provide a comprehensive discussion on all active fronts of entropic modeling. Rather, this review focuses on four computational approaches for entropy calculation: normal mode analysis, free volume theory, two-phase thermodynamics theory, and configurational entropy modeling. Normal mode analysis (NMA) is a widely used method to determine entropy by constructing partition functions from the Hessian matrix. Free volume theory accounts for the contribution of molecular volume in the calculation of translational entropy for reactions in condensed media.[11] Two-phase thermodynamics theory calculates entropy of chemical processes in condensed media through dividing the partition functions of a molecular state into gas-like and solid-like components using MD trajectories.[12] Configurational entropy modeling evaluates entropy through a direct counting approach, in which probability density functions of internal degrees of freedom are calculated using a geometric binning of molecular ensembles

sampled from MD or MC methods.[9] The theoretical basis, applications, and limitations of each approach will be discussed in the following sections. We hope the discussion can inspire more researchers to further develop and apply these methods to elucidate the entropic nature of chemical transformations.

2. Normal Mode Analysis

Normal mode analysis (NMA) assumes that a molecular system is stabilized by a series of linearly combined and non-interacting harmonic potentials. The method accounts for the entropic contribution of molecular fluctuations around a local minimum on the potential energy surface (PES). For an optimized molecular structure with N atoms, NMA constructs a $3N\ X\ 3N$ Hessian matrix to extract the information of normal modes. Each element of Hessian matrix is a second-order partial derivatives of potential energy functions over Cartesian coordinates. The diagonalization of Hessian matrix informs eigenvalues representing the local curvatures of the potential energy surface and eigenvector representing the normal mode of intramolecular vibrations. The eigenvalues of normal modes can be converted to vibrational frequencies to calculate vibrational entropy using partition functions. The rigid-body rotations and translations of the molecule are separately counted using rotational and translational partition functions, respectively. NMA is among the most popular methods available in many software packages (i.e., Gaussian,[18] Q-Chem,[19] NWChem,[20] Bio3D,[21] etc.). Below, we will introduce the technical details of NMA.

Considering a reaction in the gas phase, $A + B \rightarrow AB$, in which A and B represent reactants and AB represents a product (or a transition state complex). To calculate the entropy of each species, one would start with geometry optimization to calculate the corresponding equilibrium structures. For A, B, and AB, the optimization tracks the gradient along PES to locate

the local minima on the PES, where the gradient equals to zero. For the transition state complex, the optimization aims to locate a saddle point on the PES, which is a local maximum along one direction (i.e., the reaction coordinate) but minima for all other directions. Each optimized structure undergoes frequency analysis where translational, rotational and vibrational partition functions are constructed. Translational partition function can be represented by using Thermal de Broglie wavelength (i.e., $\Lambda = \frac{h}{\sqrt{2\pi m k_B T}}$) and the volume, V, of the system:

$$q_{trans} = \frac{V}{\Lambda^3} \qquad \textbf{eq 1}$$

where m is the mass of the molecule, T is the temperature, h is Planck constant, and k_B is Boltzmann constant.

Rotational partition function resulting from rotational degree of freedom can be represented from rotational temperature (i.e., $\Theta_{rot,k} = \frac{h^2}{8\pi^2 I_k k_B}$, where $k = x, y,$ and z Cartesian axis), which is inversely proportional to the moment of inertia, I_k:

$$q_{rot} = \frac{\pi^{1/2}}{\sigma_{rot}} \left(\frac{T^{3/2}}{(\Theta_{\mathrm{rot,x}} \Theta_{\mathrm{rot,y}} \Theta_{\mathrm{rot,z}})^{\frac{1}{2}}} \right) \qquad \textbf{eq 2}$$

where σ_{rot} is the rotational symmetry.

Vibrational partition function can be represented with the vibrational temperatures (i.e., $\Theta_{vib,K} = h\nu_K / k_B$, where K is the vibrational modes) resulting from normal mode vibrational frequencies, ν_K, identified from the diagonalization of Hessian matrix.

$$q_{vib} = \prod_K \frac{e^{-\Theta_{\mathrm{vib,K}}/2T}}{1 - e^{-\Theta_{\mathrm{vib,K}}/T}} \qquad \textbf{eq 3}$$

The electronic partition function can be simplified to the degeneracy of ground state energy level, ω_0, (i.e., $q_{elec} = \omega_0$, where ω_0), where the first and higher excited states are inaccessible under the assumption that the first electronic excitation energy is much greater than $k_B T$. Notably,

the vibronic effect should be considered when the molecular system breaks Born-Oppenheimer approximation (e.g., Jahn-Teller effects).[22]

Using partition functions (i.e., **eq 1-3**), the total entropy (i.e., contributions from translational, rotational, and vibrational modes) of each species can be calculated using **eq 4**. The overall reaction entropy and the activation of entropy can be calculated by $S_{AB} - (S_A + S_B)$ and $S_{AB^{\ddagger}} - (S_A + S_B)$, respectively.

$$S = R\left(\ln q_{trans} q_{rot} q_{vib}\right) + T\left(\frac{\delta \ln q_{trans} q_{rot} q_{vib}}{\delta T}\right)_V \quad \textbf{eq 4}$$

To account for solvent effects, implicit solvent model, which treats solvent as a continuum of uniform dielectric constant, can be used in conjunction with structural optimization or single-point energy calculation (Figure 1). The entropy associated with the overall reaction in the condensed phase can be evaluated using thermodynamic cycle, where the overall reaction entropy in the condensed phase can be obtained by the entropic variation in the gas phase combined with the entropy of solvation (Figure 1).

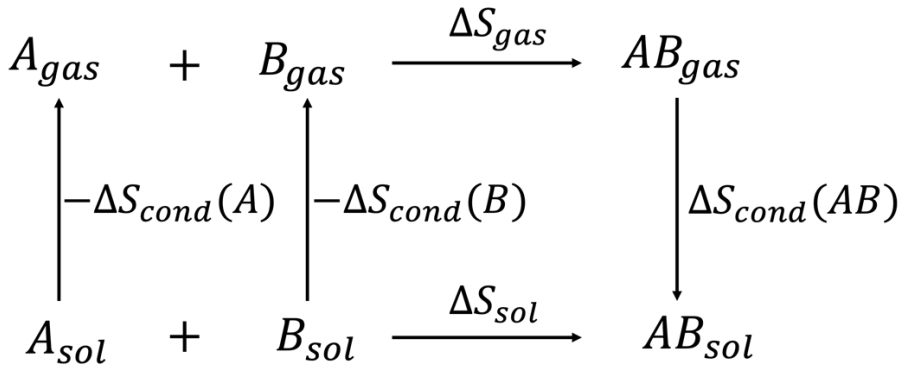

Figure 1. Thermodynamic cycle used to calculate the entropy of the reaction, $A + B \rightarrow AB$, in the solution. $\boldsymbol{\Delta S_{sol} = \Delta S_{gas} + \Delta S_{cond}(AB) - \Delta S_{cond}(A) - \Delta S_{cond}(B)}$.

In principle, NMA can be used for calculating molecular entropies under various levels of theories and methods, but its accuracy may be limited by multiple factors. First, based on the

benchmark studies by Pracht and Grimme, the mean deviation of entropy calculation is less than 1 cal mol^{-1} K^{-1} for two standard density functional theory (DFT) methods B97-3c and B3LYP-D3.[23] However, in practice, the accuracy of entropy calculations can vary significantly due the complexity of molecular systems (i.e., metal effects, multireference states, spin effects, etc.). Furthermore, insufficient DFT integration grid size can be an additional source of error that arises from overlooking the sensitivity of entropic component that are distinct from errors due to harmonic approximation.[24]

Second, NMA demands high computational cost due to the diagonalization of a $3N\ X\ 3N$ Hessian matrix. The computational complexity is on the order of N^2, which is nontrivial to calculate for systems with large number of atoms. As an approximated form of NMA, coarse-grained methods (e.g., elastic network model) have been employed to inform the large-scale collective motions for biomolecules or solvent systems,[25-28] in which the number of atoms of the whole system is usually on the scale of 10,000 to 100,000.

Third, configurational entropy derived from NMA becomes less accurate for larger and more flexible molecules. Flexible molecules involve rugged potential energy surface. Anharmonicity prevails for lower-frequency modes that feature delocalized, collective motion of large group of atoms with a longer timescale. Anharmonicity breaks the non-interacting assumption among vibrational modes and leads to larger errors in entropy calculations. To reduce this error, Truhlar and co-workers proposed quasi-harmonic method that increases the vibrational frequencies under 100 cm^{-1} to 100.[29] Later, Head-Gordon and co-workers proposed uncoupled mode approximations and improved the accuracy of entropy calculation in anharmonic systems by constructing separate one-dimensional potential energy surfaces for torsions and vibrations.[30] Besides anharmonicity, flexible molecules also involve multiple conformations that collectively

contribute to the ground state entropy and free energy. NMA derived from single optimized conformation is not theoretically adequate. To fix this error, Truhlar and co-workers developed the internal-coordinate multi-structural approximation, which is a multi-structural approach to accounting for the effects of torsional anharmonicity on entropy calculations.[31] The method involves summing torsional contributions from a list of distinguishable conformers and is shown to improve the accuracy of entropy calculations in complex molecular systems. In addition to these methods, configurational entropy calculation had been reported to calculate the total entropy change of biomacromolecule ensembles using configurational probability density functions determined from counting conformations sampled using MD or MC methods – this will be discussed in the following section (section 5).

Fourth, NMA faces problems in characterizing the entropy of molecules in the condensed phase. Quantifying entropy in such systems is challenging due to the difficulty of considering volume occupied by solvent molecules, anharmonic and diffusive motion, and solute-solvent interactions. Despite the advancement of implicit solvation models in accurately describing the solvation free energy of molecules,[32] charactering molecular entropy directly under solvent conditions remains an open question. Inclusion of explicit solvent clusters along with implicit solvent models helps improve the description of solvation energy, but how to better account for their contributions in entropy presents a major hurdle. Several computational methods have been reported to address the entropy associated with the condensed phase.[11-15] We will focus on direct entropy calculation methods for condensed media in free volume theory and two-phase thermodynamic model sections.

3. Free Volume Theory

For bimolecular reactions, translational entropy contributes significantly to the overall entropic change in the reaction. Derived from monoatomic ideal gas, Sackur-Tetrode model (i.e., **eq 5**) has been widely employed to estimate the translational entropy for molecules in the condensed media.

$$S_{trans} = R \ln\left[\left(\frac{10^{-15/2}}{N_A^4[X]}\right)\left(\frac{2\pi mRTe^{5/3}}{h^2}\right)^{3/2}\right] \qquad \textbf{eq 5}$$

In this equation, T is temperature, m is mass, h is Planck constant, N_A is the Avogadro's number, and $[X] = \frac{n}{V}$ is the molar concentration for n moles of solute in the system with a volume of V. Ideal gas model is intrinsically deficient in the description of molecular volumes and intermolecular interactions. As such, Whitesides and co-workers developed free volume theory to correct the translational entropy calculated from the Sackur-Tetrode model (Figure 2).[11] To describe the freely-accessible volume of a molecule in the condensed media (i.e., V_{free}), the theory explicitly subtracts the contribution of molecular volume (i.e., $V_{molecule}$, the volume enclosed by the van der Waals surface of the molecule) from the total volume hypothetically accessible by an ideal gas molecule (**eq 6**). The volume can be represented by a sphere or a cube.

$$V_{free} = C_{free}\left(\sqrt[3]{\frac{10^{27}}{[X]N_A}} - \sqrt[3]{V_{molecule}}\right)^3 \qquad \textbf{eq 6}$$

$V_{molecule}$ is the volume of the molecule. C_{free} is 8 or 6.3 for hard cube or sphere models, respectively.

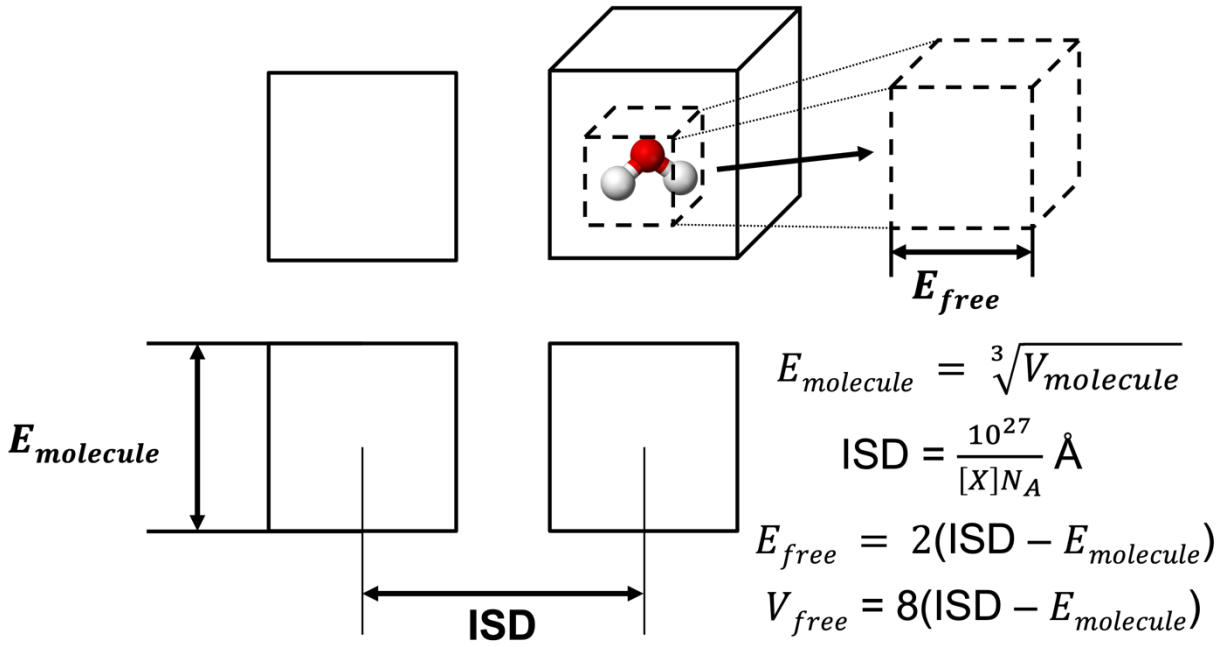

Figure 2. Free volume model addresses free volumes of pure liquids as an array of regular cubic lattices. The volume of molecule, $V_{molecule}$, can be estimated from the density of molecule and the intermolecular distances (ISD) are determined from the concentration of molecules, X. The free volume (V_{free}) available to each liquid molecule is estimated as the volume occupied by the center of mass moving in a cage defined by the intermolecular distance.

Using free volume theory, the error of translational entropy prediction for liquid-phase molecules can be significantly reduced.[11] For a reaction in the condensed phase, $A + B \rightarrow AB$, the translational components of the entropies of condensation (i.e., $\Delta \boldsymbol{S_{cond}}(\boldsymbol{AB})$, $\Delta \boldsymbol{S_{cond}}(\boldsymbol{A})$, $\Delta \boldsymbol{S_{cond}}(\boldsymbol{B})$, Figure 1) can be corrected using Sackur-Tetrode model with the V_{free} values calculated from the volume of each species. Consequently, free volume theory provides a physically informed remedy to accurately predict the translational entropy in the process of condensation. Recently, the Paton group has integrated free volume theory into the open-source Python toolkit, GoodVibes.[33] However, we should note that free volume theory is more applicable to diluted aqueous solutions with low concentration of solute. When the solute concentration

becomes higher, the free volume of solute molecules will significantly dominate the free volume of solution, and the irregular shapes of solutes hinder the estimation of free volume. These effects further complicate the estimation of solvation entropy in condensed media.

4. Two-Phase Thermodynamics Model

Besides extracting entropy from the Hessian Matrix of optimized geometries, one can also evaluate entropy from time-resolved molecular dynamics trajectories. Lin, Goddard, Pascal, and coworkers developed Two-Phase Thermodynamic (2PT) theory to predict absolute entropies of molecular fluids by evaluating density of state (DoS) distributions from the MD trajectories. As shown in Figure 3, 2PT theory represents the DoS functions of molecules in the condensed phase using a linear combination of diffusive and non-diffusive components (i.e., ideal gas and solid components, respectively). 2PT model can handle the low frequency vibrations using a measure of fluidity of the system and applies quantum statistics to the normal vibrational modes of a system (i.e., the Debye-Einstein model). Distinct from NMA, 2PT theory can account for harmonic, fluidic, and quantum effects. Based on the benchmark, the calculation of entropy is converged using one MD trajectory with 10-50 ps time scale. As such, the method is applicable to evaluate the entropy change of chemical processes in a larger-scale molecular systems with reasonable computational cost. Below, we will discuss the theoretical details of 2PT theory.

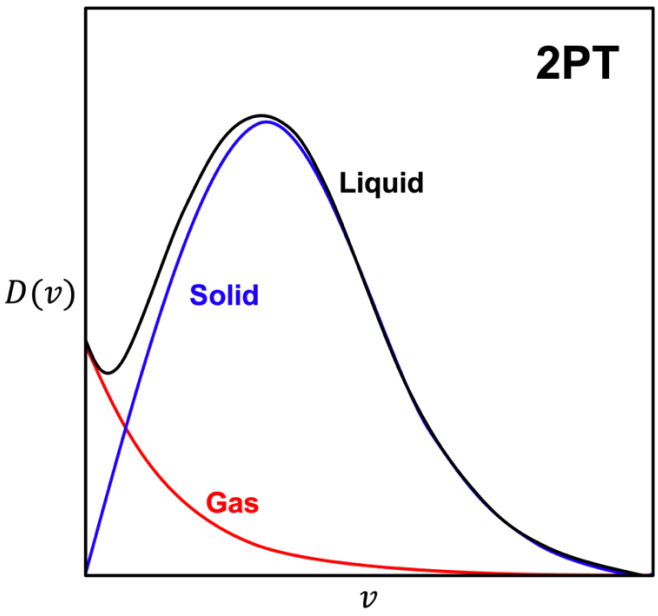

Figure 3. Typical density of state (DoS) distributions $D(v)$ of gas (red), solid (blue) and liquid (black) as a function of frequency v. The underlying assumption of two-phase thermodynamics model is that the liquid phase density of state function can be partitioned to the gas and solid components.

2PT method begins with a molecular dynamics (MD) simulation of a molecular system consisted of all target molecules and derives DoS function $D(v)$ from the Fourier transform of the corresponding velocity autocorrelation functions. The DoS functions of fluid molecules, which contain the information of translation, rotation, and intramolecular vibration motions, are partitioned into the solid-like and gas-like components. The zero-frequency intensity $D(v = 0)$ corresponds to the diffusive modes of the system. For solid-like components, the DoS function can be represented as the Debye-Einstein model, in which the system is treated as a continuous collection of noninteracting quantum harmonic oscillators (i.e., $D(0) = 0$). For gases, the DoS decays exponentially with frequency, which represents anharmonicity and diffusivity of the system (i.e., $D(0) > 0$).

The molecules in MD simulation are equilibrated for 1-2 ns. Atomic velocities are saved every 4 fs. Atomic velocities are decomposed into translational, rotational, and vibrational components using eq 7 for atom j in the k direction ($k = x, y,$ and z in the Cartesian coordinate).

$v_j^k(t) = v_{j,trans}^k(t) + v_{j,rot}^k(t) + v_{j,vib}^k(t)$ **eq 7**

Translational velocity of atom j is represented by the center of mass velocity of the molecule in which the atom j resides. Rotational velocity can be represented by the cross product of the position vector of atom j and the angular velocity: $\vec{\omega} \times \vec{r_j}$, where $\vec{r_j}$ is the position vector of atom j to the center of mass of the molecule and $\vec{\omega}$ is the angular velocity determined from $\vec{\boldsymbol{L}} = \sum m_j(\vec{r_j} \times \vec{v_j}) = \boldsymbol{I}\vec{\omega}$. Vibrational velocity can be obtained from $v_{j,vib}^k(t) = v_j^k(t) - v_{j,trans}^k(t) - v_{j,rot}^k(t)$.

The DoS function $D(v)$ is defined as the mass weighted sum of the atomic spectral densities $D(v) = \frac{2}{k_B T}\sum_{j=1}^{N}\sum_{k=1}^{3} m_j s_j^k(v)$, where m_j is the mass of atom j and N is the total number of atoms in the system. The spectral density $s_j^k(v)$ of atom j in the k direction ($k = x, y,$ and z in the Cartesian coordinate) is defined as the square of the Fourier transform of the velocities $s_j^k(v) = \lim_{\tau-\infty} \frac{1}{2\tau}\left|\int_{-\tau}^{\tau} v_j^k(t) e^{-i2\pi v t} dt\right|^2$, where $v_j^k(t)$is the k-component of the velocity vector of atom j at time t. Therefore, the DoS function can be expressed as

$D_{trans}(v) = \frac{2}{k_B T}\sum_{j=1}^{N}\sum_{k=1}^{3} m_j s_j^k(v) = \frac{1}{k_B T}\sum_{j=1}^{N}\sum_{k=1}^{3} \frac{m_j}{\tau}\left|\int_{-\tau}^{\tau} v_{j,trans}^k(t) e^{-i2\pi v t} dt\right|^2 = D_{trans}^{gas}(v) + D_{trans}^{solid}(v)$ **eq 8**

$D_{rot}(v) = \frac{2}{k_B T}\sum_{j=1}^{N}\sum_{k=1}^{3} m_j s_j^k(v) = \frac{1}{k_B T}\sum_{l=1}^{M}\sum_{k=1}^{3} \frac{I_l^k}{\tau}\left|\int_{-\tau}^{\tau} \omega_l^k(t) e^{-i2\pi v t} dt\right|^2 = D_{rot}^{gas}(v) + D_{rot}^{solid}(v)$ **eq 9**

$$D_{vib}(v) = \frac{2}{k_B T}\sum_{j=1}^{N}\sum_{k=1}^{3} m_j s_j^k(v) = \frac{1}{k_B T}\sum_{j=1}^{N}\sum_{k=1}^{3}\frac{m_j}{\tau}\left|\int_{-\tau}^{\tau} v_{j,vib}^k(t)e^{-i2\pi\nu t}dt\right|^2 = D_{vib}^{solid}(v)$$

eq 10

In **eq 9**, M is the total number of molecules for the rotational component, and ω_l^k and I_l^k are the k-th principle angular momentum and moment of inertia of molecule, respectively. Under the assumption that all the normal modes are harmonic, the vibrational DoS function of the gas component can be neglected.

In the condensed phase, the motions associated with the low frequency modes mediate the fluidicity of the system. Using diffusivity obtained from MD simulation (under the framework of NVT ensemble), the fluidicity can be determined to characterize translational and rotational DoS functions of the gas component using **eq 11**.

$$2\Delta^{-9/2} f_{mode}^{15/2} - 6\Delta^{-3} f_{mode}^{5} - \Delta^{-3/2} f_{mode}^{7/2} + 6\Delta^{-3/2} f_{mode}^{5/2} + 2f_{mode} - 2 = 0 \qquad \textbf{eq 11}$$

Diffusivity constant, Δ, can be defined as:

$$\Delta(t, V, N, m, D_{mode}^0) = \frac{2D_{mode}^0}{9N}\left(\frac{\pi k_B T}{m}\right)^{1/2}\left(\frac{N}{V}\right)^{1/3}\left(\frac{6}{\pi}\right)^{2/3} \qquad \textbf{eq 12}$$

where mode = translational and rotational.

$$D_{mode}^{gas}(v) = \frac{D_{mode}^0}{1+\left[\frac{\pi D_{mode}^0 v}{6 f_{mode} N}\right]^2} \qquad \textbf{eq 13}$$

As translational and rotational DoS functions of the gas component are completely determined, the solid components can be obtained by subtracting $D_{mode}^{gas}(v)$ from the total DoS functions $D_{mode}(v)$ (i.e., $D_{mode}^{solid}(v) = D_{mode}(v) - D_{mode}^{gas}(v)$). With demonstrated 2PT decomposition of the density of states, the entropy of the system is determined as the sum of the gas and solid contributions:

$$S_{trans} = k_B\left[\int_0^\infty dv D_{trans}^{solid}(v) W_S^{solid}(v) + \int_0^\infty dv D_{trans}^{gas}(v) W_{trans,S}^{gas}(v)\right] \qquad \textbf{eq 14}$$

$$S_{rot} = k_B\left[\int_0^\infty dv D_{rot}^{solid}(v) W_S^{solid}(v) + \int_0^\infty dv D_{rot}^{gas}(v) W_{rot,S}^{gas}(v)\right] \quad \textbf{eq 15}$$

$$S_{vib} = k_B \int_0^\infty dv D_{vib}(v) W_S^{solid}(v) \quad \textbf{eq 16}$$

$$W_S^{solid}(v) = \frac{\beta h v}{\exp(\beta h v) - 1} - \ln[1 - \exp(-\beta h v)] \quad \textbf{eq 17}$$

where the weighting functions for solid component, $W_S^{solid}(v)$, are modeled with harmonic oscillators. The weighting function of the translational motion of gas component is assumed to be that of hard spheres,[34]

$$W_{trans,S}^{gas}(v) = W_S^{HS}(v) = \frac{1}{3}\frac{S^{HS}}{k_B} = \frac{1}{3}\left\{\frac{5}{2} + \ln\left[\left(\frac{2\pi m k_B T}{h^2}\right)^{3/2} \frac{V}{f_{trans} N} z(y)\right] + \frac{y(3y-4)}{(1-y)^2}\right\} \quad \textbf{eq 18}$$

$$z(y) = \frac{1 + y + y^2 - y^3}{(1-y)^3} \quad \textbf{eq 19}$$

where S^{HS} is the hard sphere entropy and $y = f_{trans}^{5/2} / \Delta^{3/2}$. $z(y)$ is the compressibility factor derived from Carnahan-Starling equation of state of hard sphere gasses. The weighting function of the rotational motion of gas component is

$$W_{rot,S}^{gas}(v) = \frac{1}{3}\frac{S^R}{k_B} = \frac{1}{3}\left\{\ln\left[\frac{\pi^{1/2} e^{3/2}}{\sigma}\left(\frac{T^3}{\Theta_A \Theta_B \Theta_C}\right)^{1/2}\right]\right\} \quad \textbf{eq 20}$$

where S^R is the rotational entropy of a rigid body with rotational temperature $\Theta_A = h^2 / 8\pi^2 I_A k_B$.

By partitioning liquid density of state function into gas and solid components, 2PT model separately treats harmonic, fluidic, and quantum effects to accurately calculate absolute entropy for liquid-phase molecules. Furthermore, 2PT model can be applied to various range of temperature and density. For instance, Lin et al. demonstrated the accurate prediction of entropy of water along the saturation curve.[12] 2PT model has also been employed to characterize entropy of water dynamics involved in enzymatic reactions,[35] water-carbon nanomaterial interfaces,[36-39] amorphous polyethylene glycol-water mixtures,[40] and biological systems.[41, 42] Furthermore,

besides small molecules such as water and carbon dioxide,[43] 2PT model has been recently suggested to accurately calculate the absolute entropy of flexible molecules in condensed phase.[44]

5. Configurational Entropy Calculation

Configurational entropy calculation determines the overall entropy of a molecule by analyzing the probability density function (PDFs) of the internal degrees of freedom obtained from MD or MC simulations of molecular ensembles. Unlike NMA, which extracts vibrational modes from a Hessian matrix of optimized structures, configurational entropy calculation builds configurational PDFs of internal coordinates (i.e., bond, angle, and torsion angle) from a collection of sampled structures. High-dimensional configurational PDFs can be estimated using a combination of Generalized Kirkwood Superposition Approximation (GKSA)[45, 46] and the Maximum Information Spanning Tree (MIST) approximation.[47, 48] GKSA helps overcome the challenge of high dimensionality by approximating the high-order configurational PDF using pairwise MI terms. MIST approximation removes small MI terms to prevent overestimation of full-dimensional entropy.

The total entropy of a molecule can be partitioned into the momentum and spatial components where in isothermal condition, the momentum component is constant and can be not considered. Therefore, the total entropy of a single molecule can be described by spatial component as shown in **eq 21**,

$$S_{3N}^{spatial} = -k_B \int \partial q_1 \dots \partial q_{3N} \rho(q_1 \dots q_{3N}) \ln[\rho(q_1 \dots q_{3N})] \quad \textbf{eq 21}$$

where ρ is the configurational probability density function (PDF), q_i terms are the spatial degrees of freedom (DoFs), and $3N$ is the total number of DoFs in Cartesian coordinate system for N atoms. The spatial component can be further decomposed into the configurational and roto-translational components; under a rigid-body roto-translational coordinate transformation, external roto-

translational components is not considered. Therefore, the configurational entropy refers to the spatial DoFs, with the momentum and external roto-translational contributions removed.

Configurational entropy calculation starts by converting the molecular configurations in dynamic trajectories from Cartesian coordinates to internal coordinates (Z-matrix), which naturally excludes rotational and translational degrees of freedom. The internal coordinate system consists of bond lengths, angles, and torsional angles; for N atoms, the total number of DoFs, in which there can be $N-1$ bonds, $N-2$ angles, and $N-3$ torsional angles (i.e., $b_1, \dots, b_{N-1}, \theta_1, \dots, \theta_{N-2}, \phi_1, \dots, \phi_{N-3}$), equals to $3N-6$ vibrational DoFs in Cartesian coordinate system. Using histogram-based methods, 1D and 2D histograms can be obtained to estimate the configurational PDFs, which are used to calculate 1D and 2D entropies in the following equations:

$$S_{X_i} = -\sum_k \rho_{X_i}[k] \ln\left(\frac{\rho_{X_i}[k]}{J(X_i[k])h_{X_i}}\right) \qquad \textbf{eq 22}$$

$$S_{X_i,X_j} = -\sum_{k,l} \rho_{X_i,X_j}[k,l] \ln\left(\frac{\rho_{X_i,X_j}[k,l]}{J(X_i[k])J(X_j[l])h_{X_i}h_{X_j}}\right) \qquad \textbf{eq 23}$$

where $j \in [i+1, 3N-6]$, $X_i, X_j \in [b_1, \dots, b_{N-1}, \theta_1, \dots, \theta_{N-2}, \phi_1, \dots, \phi_{N-3}]$, k and l are indices of histograms, h_{X_i} and h_{X_j} are the width of the bins, and $J(X_i[k])$ and $J(X_j[l])$ are the Jacobian determinants for the internal coordinates as defined below:

$$J(b) = b^2 \qquad \textbf{eq 24}$$

$$J(\theta) = \sin(\theta) \qquad \textbf{eq 25}$$

$$J(\phi) = 1 \qquad \textbf{eq 26}$$

The total configurational entropy is computed with MI terms from GKSA and the MIST approximation as shown in **eq 27**,

$$S_{3N-6}^{MIST}(X_1, \dots, X_{3N-6}) = \sum_{i=1}^{3N-6}\left[S_1(X_i) - \max_{j\in\{1,\dots,i-1\}} I_2(X_i; X_j)\right] \qquad \textbf{eq 27}$$

where X_i is DoF and $I_2(X_i; X_j) \equiv S_1(X_i) + S_1(X_j) - S_2(X_i, X_j)$ is the mutual information (MI) that represents the interdependency among DoFs.

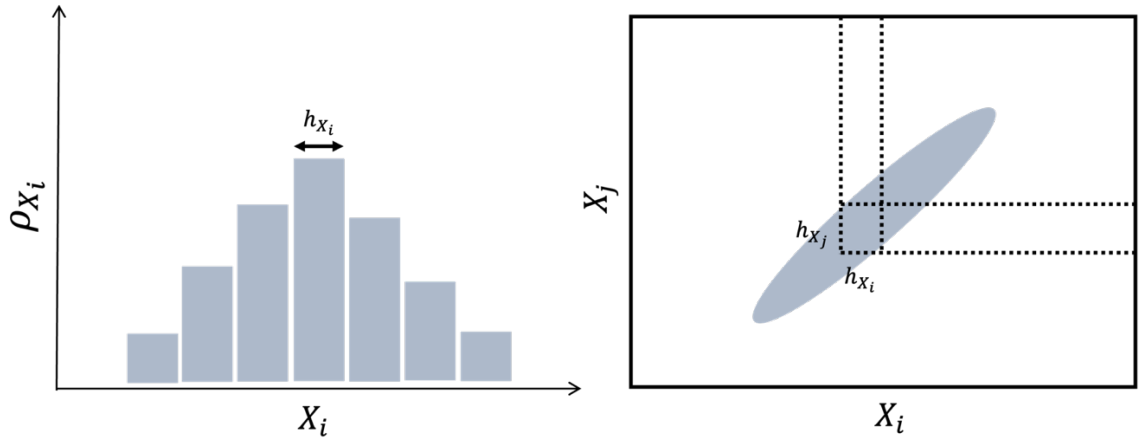

Figure 4. Illustration of 1-dimensional (left) and 2-dimensional (right) histograms using DoFs (i.e., X_i, X_j). Each represents the probability density distribution, where h_{X_i} and h_{X_j} represent the widths of bins.

Configurational entropy calculation is used to determine the total entropy change of flexible and moderate-sized molecules by creating configurational probability density functions (PDFs) based on fully equilibrated MD simulation trajectories. The advantage of this approach is its ability to effectively account for anharmonic and coupling effects using configurational PDFs and mutual information between degrees of freedom. Furthermore, unlike the Two-Phase Thermodynamics (2PT) model, which only captures entropy at a sub-nanosecond time scale, configurational entropy calculations can capture conformational changes over long-time scales and provide a more comprehensive understanding of the entropy associated with biomolecular processes.

Based on the framework of configurational entropy calculation, our group previously developed entropic path sampling (EPS) to evaluate the change of entropy along reaction path using a collection of reaction dynamic trajectories.[49] Along the post-transition-state reaction path,

the reaction dynamic trajectories are divided into structural ensembles that are consecutively spaced along a specific geometric range for the reacting bond. For each structural ensemble, its configurational entropy is computed to analyze the entropic path. Furthermore, configurational PDFs can be decomposed into structural moieties for entropy decomposition analysis.[50] This approach can be potentially used to understand the entropic origin behind the selectivity of organic reaction dynamics.[51]

However, the configurational entropy cannot characterize the entropy of the many-body system, where the solvent-mediated interaction entropy remains uncertain. Configurational entropy calculation can address the entropy of condensation by calculating the entropy difference of the target molecule between gas phase and condensed phase simulations. However, the total entropy change of the molecular system cannot be represented by simply adding configurational entropies of molecules and solute-solvent interaction entropy calculation is limited with increasing number of molecules in the system.

Conclusion

In this review, we focus on the discussion of four computational methods used to calculate entropy in chemical processes, including their theoretical foundation, computational applications, and limitations. Normal mode analysis derives translational, rotational, and vibrational entropy based on the optimized structure's Hessian matrix. The free volume theory improves the calculation of translational entropy during chemical condensation by incorporating the contribution of molecular volume. The two-phase thermodynamics model calculates the absolute entropy of the condensed phase by dividing the density of state function into the contributions of gas- and solid-like components. Configurational entropy calculation determines the entropy of

large and flexible molecules using probability density functions derived from molecular ensembles built by molecular dynamics or Monte Carlo simulations.

These theoretical and computational advances enable researchers to gain tremendous insights into the conformational changes that occur during chemical reactions. The immediate challenge is to increase the accuracy of these methods through the use of more accurate potential energy functions, enhanced sampling of conformational space, and more sophisticated computational models for complex molecular systems. The incorporation of data-driven modeling also provides tremendous opportunities to further the accuracy of entropy calculations.[52] It is hoped that this review will inspire further development and application of these methods to deepen our understanding of the entropic nature of chemical processes.

AUTHOR INFORMATION

Notes

The authors declare no competing financial interest.

ACKNOWLEDGMENTS

This research was supported by the startup grant from Vanderbilt University.

References

1. Dragan, A. I.; Read, C. M.; Crane-Robinson, C., Enthalpy–entropy compensation: the role of solvation. *European Biophysics Journal* **2017,** *46* (4), 301-308.
2. Lumry, R.; Rajender, S., Enthalpy–entropy compensation phenomena in water solutions of proteins and small molecules: A ubiquitous properly of water. *Biopolymers* **1970,** *9* (10), 1125-1227.
3. Meijer, E. W., Jacobus Henricus van 't Hoff; Hundred Years of Impact on Stereochemistry in the Netherlands. *Angewandte Chemie International Edition* **2001,** *40* (20), 3783-3789.
4. Saito, N.; Ishizaki, T.; Fuwa, A., Kinetics of SiHCl₃ and SiCl₄ Evolution in Si(s)–HCl(g) System Simulated by Ab-initio MO. *Materials Transactions, JIM* **2000,** *41* (3), 383-392.
5. Leavitt, S.; Freire, E., Direct measurement of protein binding energetics by isothermal titration calorimetry. *Current Opinion in Structural Biology* **2001,** *11* (5), 560-566.

6. Bruylants, G.; Wouters, J.; Michaux, C., Differential Scanning Calorimetry in Life Science: Thermodynamics, Stability, Molecular Recognition and Application in Drug Design. *Current Medicinal Chemistry* **2005,** *12* (17), 2011-2020.
7. Armstrong, A. A.; Amzel, L. M., Role of Entropy in Increased Rates of Intramolecular Reactions. *Journal of the American Chemical Society* **2003,** *125* (47), 14596-14602.
8. Tidor, B.; Karplus, M., The contribution of cross-links to protein stability: A normal mode analysis of the configurational entropy of the native state. *Proteins: Structure, Function, and Bioinformatics* **1993,** *15* (1), 71-79.
9. Fleck, M.; Polyansky, A. A.; Zagrovic, B., PARENT: A Parallel Software Suite for the Calculation of Configurational Entropy in Biomolecular Systems. *Journal of Chemical Theory and Computation* **2016,** *12* (4), 2055-2065.
10. Meirovitch, H., Recent developments in methodologies for calculating the entropy and free energy of biological systems by computer simulation. *Current Opinion in Structural Biology* **2007,** *17* (2), 181-186.
11. Mammen, M.; Shakhnovich, E. I.; Deutch, J. M.; Whitesides, G. M., Estimating the Entropic Cost of Self-Assembly of Multiparticle Hydrogen-Bonded Aggregates Based on the Cyanuric Acid·Melamine Lattice. *The Journal of Organic Chemistry* **1998,** *63* (12), 3821-3830.
12. Lin, S.-T.; Maiti, P. K.; Goddard, W. A., III, Two-Phase Thermodynamic Model for Efficient and Accurate Absolute Entropy of Water from Molecular Dynamics Simulations. *The Journal of Physical Chemistry B* **2010,** *114* (24), 8191-8198.
13. Sindhikara, D. J.; Hirata, F., Analysis of Biomolecular Solvation Sites by 3D-RISM Theory. *The Journal of Physical Chemistry B* **2013,** *117* (22), 6718-6723.
14. Velez-Vega, C.; McKay, D. J. J.; Kurtzman, T.; Aravamuthan, V.; Pearlstein, R. A.; Duca, J. S., Estimation of Solvation Entropy and Enthalpy via Analysis of Water Oxygen–Hydrogen Correlations. *Journal of Chemical Theory and Computation* **2015,** *11* (11), 5090-5102.
15. Moghaddam, M. S.; Shimizu, S.; Chan, H. S., Temperature Dependence of Three-Body Hydrophobic Interactions: Potential of Mean Force, Enthalpy, Entropy, Heat Capacity, and Nonadditivity. *Journal of the American Chemical Society* **2005,** *127* (1), 303-316.
16. Huang, D. M.; Chandler, D., Temperature and length scale dependence of hydrophobic effects and their possible implications for protein folding. *Proceedings of the National Academy of Sciences* **2000,** *97* (15), 8324-8327.
17. Bui, T.; Frampton, H.; Huang, S.; Collins, I. R.; Striolo, A.; Michaelides, A., Water/oil interfacial tension reduction – an interfacial entropy driven process. *Physical Chemistry Chemical Physics* **2021,** *23* (44), 25075-25085.
18. Frisch, M. J.; Trucks, G. W.; Schlegel, H. B.; Scuseria, G. E.; Robb, M. A.; Cheeseman, J. R.; Scalmani, G.; Barone, V.; Petersson, G. A.; Nakatsuji, H.; Li, X.; Caricato, M.; Marenich, A. V.; Bloino, J.; Janesko, B. G.; Gomperts, R.; Mennucci, B.; Hratchian, H. P.; Ortiz, J. V.; Izmaylov, A. F.; Sonnenberg, J. L.; Williams; Ding, F.; Lipparini, F.; Egidi, F.; Goings, J.; Peng, B.; Petrone, A.; Henderson, T.; Ranasinghe, D.; Zakrzewski, V. G.; Gao, J.; Rega, N.; Zheng, G.; Liang, W.; Hada, M.; Ehara, M.; Toyota, K.; Fukuda, R.; Hasegawa, J.; Ishida, M.; Nakajima, T.; Honda, Y.; Kitao, O.; Nakai, H.; Vreven, T.; Throssell, K.; Montgomery Jr., J. A.; Peralta, J. E.; Ogliaro, F.; Bearpark, M. J.; Heyd, J. J.; Brothers, E. N.; Kudin, K. N.; Staroverov, V. N.; Keith, T. A.; Kobayashi, R.; Normand, J.; Raghavachari, K.; Rendell, A. P.; Burant, J. C.; Iyengar, S. S.; Tomasi, J.; Cossi, M.; Millam, J. M.; Klene, M.; Adamo, C.; Cammi, R.; Ochterski, J. W.; Martin, R. L.; Morokuma, K.; Farkas, O.; Foresman, J. B.; Fox, D. J. *Gaussian 16 Rev. C.01*, Wallingford, CT, 2016.

19. Shao, Y.; Gan, Z.; Epifanovsky, E.; Gilbert, A. T. B.; Wormit, M.; Kussmann, J.; Lange, A. W.; Behn, A.; Deng, J.; Feng, X.; Ghosh, D.; Goldey, M.; Horn, P. R.; Jacobson, L. D.; Kaliman, I.; Khaliullin, R. Z.; Kuś, T.; Landau, A.; Liu, J.; Proynov, E. I.; Rhee, Y. M.; Richard, R. M.; Rohrdanz, M. A.; Steele, R. P.; Sundstrom, E. J.; Woodcock, H. L.; Zimmerman, P. M.; Zuev, D.; Albrecht, B.; Alguire, E.; Austin, B.; Beran, G. J. O.; Bernard, Y. A.; Berquist, E.; Brandhorst, K.; Bravaya, K. B.; Brown, S. T.; Casanova, D.; Chang, C.-M.; Chen, Y.; Chien, S. H.; Closser, K. D.; Crittenden, D. L.; Diedenhofen, M.; DiStasio, R. A.; Do, H.; Dutoi, A. D.; Edgar, R. G.; Fatehi, S.; Fusti-Molnar, L.; Ghysels, A.; Golubeva-Zadorozhnaya, A.; Gomes, J.; Hanson-Heine, M. W. D.; Harbach, P. H. P.; Hauser, A. W.; Hohenstein, E. G.; Holden, Z. C.; Jagau, T.-C.; Ji, H.; Kaduk, B.; Khistyaev, K.; Kim, J.; Kim, J.; King, R. A.; Klunzinger, P.; Kosenkov, D.; Kowalczyk, T.; Krauter, C. M.; Lao, K. U.; Laurent, A. D.; Lawler, K. V.; Levchenko, S. V.; Lin, C. Y.; Liu, F.; Livshits, E.; Lochan, R. C.; Luenser, A.; Manohar, P.; Manzer, S. F.; Mao, S.-P.; Mardirossian, N.; Marenich, A. V.; Maurer, S. A.; Mayhall, N. J.; Neuscamman, E.; Oana, C. M.; Olivares-Amaya, R.; O'Neill, D. P.; Parkhill, J. A.; Perrine, T. M.; Peverati, R.; Prociuk, A.; Rehn, D. R.; Rosta, E.; Russ, N. J.; Sharada, S. M.; Sharma, S.; Small, D. W.; Sodt, A.; Stein, T.; Stück, D.; Su, Y.-C.; Thom, A. J. W.; Tsuchimochi, T.; Vanovschi, V.; Vogt, L.; Vydrov, O.; Wang, T.; Watson, M. A.; Wenzel, J.; White, A.; Williams, C. F.; Yang, J.; Yeganeh, S.; Yost, S. R.; You, Z.-Q.; Zhang, I. Y.; Zhang, X.; Zhao, Y.; Brooks, B. R.; Chan, G. K. L.; Chipman, D. M.; Cramer, C. J.; Goddard, W. A.; Gordon, M. S.; Hehre, W. J.; Klamt, A.; Schaefer, H. F.; Schmidt, M. W.; Sherrill, C. D.; Truhlar, D. G.; Warshel, A.; Xu, X.; Aspuru-Guzik, A.; Baer, R.; Bell, A. T.; Besley, N. A.; Chai, J.-D.; Dreuw, A.; Dunietz, B. D.; Furlani, T. R.; Gwaltney, S. R.; Hsu, C.-P.; Jung, Y.; Kong, J.; Lambrecht, D. S.; Liang, W.; Ochsenfeld, C.; Rassolov, V. A.; Slipchenko, L. V.; Subotnik, J. E.; Van Voorhis, T.; Herbert, J. M.; Krylov, A. I.; Gill, P. M. W.; Head-Gordon, M., Advances in molecular quantum chemistry contained in the Q-Chem 4 program package. *Molecular Physics* **2015,** *113* (2), 184-215.

20. Aprà, E.; Bylaska, E. J.; de Jong, W. A.; Govind, N.; Kowalski, K.; Straatsma, T. P.; Valiev, M.; van Dam, H. J. J.; Alexeev, Y.; Anchell, J.; Anisimov, V.; Aquino, F. W.; Atta-Fynn, R.; Autschbach, J.; Bauman, N. P.; Becca, J. C.; Bernholdt, D. E.; Bhaskaran-Nair, K.; Bogatko, S.; Borowski, P.; Boschen, J.; Brabec, J.; Bruner, A.; Cauët, E.; Chen, Y.; Chuev, G. N.; Cramer, C. J.; Daily, J.; Deegan, M. J. O.; Dunning, T. H.; Dupuis, M.; Dyall, K. G.; Fann, G. I.; Fischer, S. A.; Fonari, A.; Früchtl, H.; Gagliardi, L.; Garza, J.; Gawande, N.; Ghosh, S.; Glaesemann, K.; Götz, A. W.; Hammond, J.; Helms, V.; Hermes, E. D.; Hirao, K.; Hirata, S.; Jacquelin, M.; Jensen, L.; Johnson, B. G.; Jónsson, H.; Kendall, R. A.; Klemm, M.; Kobayashi, R.; Konkov, V.; Krishnamoorthy, S.; Krishnan, M.; Lin, Z.; Lins, R. D.; Littlefield, R. J.; Logsdail, A. J.; Lopata, K.; Ma, W.; Marenich, A. V.; Martin del Campo, J.; Mejia-Rodriguez, D.; Moore, J. E.; Mullin, J. M.; Nakajima, T.; Nascimento, D. R.; Nichols, J. A.; Nichols, P. J.; Nieplocha, J.; Otero-de-la-Roza, A.; Palmer, B.; Panyala, A.; Pirojsirikul, T.; Peng, B.; Peverati, R.; Pittner, J.; Pollack, L.; Richard, R. M.; Sadayappan, P.; Schatz, G. C.; Shelton, W. A.; Silverstein, D. W.; Smith, D. M. A.; Soares, T. A.; Song, D.; Swart, M.; Taylor, H. L.; Thomas, G. S.; Tipparaju, V.; Truhlar, D. G.; Tsemekhman, K.; Van Voorhis, T.; Vázquez-Mayagoitia, Á.; Verma, P.; Villa, O.; Vishnu, A.; Vogiatzis, K. D.; Wang, D.; Weare, J. H.; Williamson, M. J.; Windus, T. L.; Woliński, K.; Wong, A. T.; Wu, Q.; Yang, C.; Yu, Q.; Zacharias, M.; Zhang, Z.; Zhao, Y.; Harrison, R. J., NWChem: Past, present, and future. *The Journal of Chemical Physics* **2020,** *152* (18), 184102.

21. Grant, B. J.; Rodrigues, A. P. C.; ElSawy, K. M.; McCammon, J. A.; Caves, L. S. D., Bio3d: an R package for the comparative analysis of protein structures. *Bioinformatics* **2006,** *22* (21), 2695-2696.
22. Kayi, H.; Garcia-Fernandez, P.; Bersuker, I. B.; Boggs, J. E., Deviations from Born–Oppenheimer Theory in Structural Chemistry: Jahn–Teller, Pseudo Jahn–Teller, and Hidden Pseudo Jahn–Teller Effects in C3H3 and C3H3–. *The Journal of Physical Chemistry A* **2013,** *117* (36), 8671-8679.
23. Pracht, P.; Grimme, S., Calculation of absolute molecular entropies and heat capacities made simple. *Chemical Science* **2021,** *12* (19), 6551-6568.
24. Bootsma, A.; Wheeler, S., *Popular Integration Grids Can Result in Large Errors in DFT-Computed Free Energies*. 2019.
25. Tirion, M. M., Large Amplitude Elastic Motions in Proteins from a Single-Parameter, Atomic Analysis. *Physical Review Letters* **1996,** *77* (9), 1905-1908.
26. Bahar, I.; Atilgan, A. R.; Erman, B., Direct evaluation of thermal fluctuations in proteins using a single-parameter harmonic potential. *Folding and Design* **1997,** *2* (3), 173-181.
27. Hinsen, K., Analysis of domain motions by approximate normal mode calculations. *Proteins: Structure, Function, and Bioinformatics* **1998,** *33* (3), 417-429.
28. Xu, B.; Shen, H.; Zhu, X.; Li, G., Fast and accurate computation schemes for evaluating vibrational entropy of proteins. *Journal of Computational Chemistry* **2011,** *32* (15), 3188-3193.
29. Ribeiro, R. F.; Marenich, A. V.; Cramer, C. J.; Truhlar, D. G., Use of Solution-Phase Vibrational Frequencies in Continuum Models for the Free Energy of Solvation. *The Journal of Physical Chemistry B* **2011,** *115* (49), 14556-14562.
30. Li, Y.-P.; Bell, A. T.; Head-Gordon, M., Thermodynamics of Anharmonic Systems: Uncoupled Mode Approximations for Molecules. *Journal of Chemical Theory and Computation* **2016,** *12* (6), 2861-2870.
31. Zheng, J.; Yu, T.; Papajak, E.; Alecu, I. M.; Mielke, S. L.; Truhlar, D. G., Practical methods for including torsional anharmonicity in thermochemical calculations on complex molecules: The internal-coordinate multi-structural approximation. *Physical Chemistry Chemical Physics* **2011,** *13* (23), 10885-10907.
32. Marenich, A. V.; Cramer, C. J.; Truhlar, D. G., Universal Solvation Model Based on Solute Electron Density and on a Continuum Model of the Solvent Defined by the Bulk Dielectric Constant and Atomic Surface Tensions. *The Journal of Physical Chemistry B* **2009,** *113* (18), 6378-6396.
33. Luchini, G. a. A.-R., JV and Funes-Ardoiz, I and Paton, RS, GoodVibes: automated thermochemistry for heterogeneous computational chemistry data [version 1; peer review: 2 approved with reservations]. *F1000Research* **2020,** *9* (291).
34. Lin, S.-T.; Blanco, M.; Goddard, W. A., The two-phase model for calculating thermodynamic properties of liquids from molecular dynamics: Validation for the phase diagram of Lennard-Jones fluids. *The Journal of Chemical Physics* **2003,** *119* (22), 11792-11805.
35. Belsare, S.; Pattni, V.; Heyden, M.; Head-Gordon, T., Solvent Entropy Contributions to Catalytic Activity in Designed and Optimized Kemp Eliminases. *The Journal of Physical Chemistry B* **2018,** *122* (21), 5300-5307.
36. Varanasi, S. R.; Subramanian, Y.; Bhatia, S. K., High Interfacial Barriers at Narrow Carbon Nanotube–Water Interfaces. *Langmuir* **2018,** *34* (27), 8099-8111.

37. Pascal, T. A.; Goddard, W. A.; Jung, Y., Entropy and the driving force for the filling of carbon nanotubes with water. *Proceedings of the National Academy of Sciences* **2011,** *108* (29), 11794-11798.
38. Chen, Z.; Yang, J.; Ma, C.; Zhou, K.; Jiao, S., Continuous Water Filling in a Graphene Nanochannel: A Molecular Dynamics Study. *The Journal of Physical Chemistry B* **2021,** *125* (34), 9824-9833.
39. Pascal, T. A.; Goddard, W. A., III, Entropic Stabilization of Water at Graphitic Interfaces. *The Journal of Physical Chemistry Letters* **2021,** *12* (37), 9162-9168.
40. Shin, H.; Pascal, T. A.; Goddard, W. A., III; Kim, H., Scaled Effective Solvent Method for Predicting the Equilibrium Ensemble of Structures with Analysis of Thermodynamic Properties of Amorphous Polyethylene Glycol–Water Mixtures. *The Journal of Physical Chemistry B* **2013,** *117* (3), 916-927.
41. Vasumathi, V.; Maiti, P. K., Complexation of siRNA with Dendrimer: A Molecular Modeling Approach. *Macromolecules* **2010,** *43* (19), 8264-8274.
42. Nandy, B.; Maiti, P. K., DNA Compaction by a Dendrimer. *The Journal of Physical Chemistry B* **2011,** *115* (2), 217-230.
43. Huang, S.-N.; Pascal, T. A.; Goddard, W. A., III; Maiti, P. K.; Lin, S.-T., Absolute Entropy and Energy of Carbon Dioxide Using the Two-Phase Thermodynamic Model. *Journal of Chemical Theory and Computation* **2011,** *7* (6), 1893-1901.
44. Lai, P.-K.; Lin, S.-T., Rapid determination of entropy for flexible molecules in condensed phase from the two-phase thermodynamic model. *RSC Advances* **2014,** *4* (19), 9522-9533.
45. Singer, A., Maximum entropy formulation of the Kirkwood superposition approximation. *The Journal of Chemical Physics* **2004,** *121* (8), 3657-3666.
46. Killian, B. J.; Yundenfreund Kravitz, J.; Gilson, M. K., Extraction of configurational entropy from molecular simulations via an expansion approximation. *The Journal of Chemical Physics* **2007,** *127* (2), 024107.
47. King, B. M.; Tidor, B., MIST: Maximum Information Spanning Trees for dimension reduction of biological data sets. *Bioinformatics* **2009,** *25* (9), 1165-1172.
48. King, B. M.; Silver, N. W.; Tidor, B., Efficient Calculation of Molecular Configurational Entropies Using an Information Theoretic Approximation. *The Journal of Physical Chemistry B* **2012,** *116* (9), 2891-2904.
49. Qin, Z.-X.; Tremblay, M.; Hong, X.; Yang, Z. J., Entropic Path Sampling: Computational Protocol to Evaluate Entropic Profile along a Reaction Path. *The Journal of Physical Chemistry Letters* **2021,** *12* (43), 10713-10719.
50. Shin, W.; Ran, X.; Wang, X.; Yang, Z., *Accelerated Entropic Path Sampling Elucidates Entropic Effects in Mediating the Ambimodal Selectivity of NgnD-Catalyzed Diels–Alder Reaction*. 2022.
51. Tantillo, D. J., Portable Models for Entropy Effects on Kinetic Selectivity. *Journal of the American Chemical Society* **2022,** *144* (31), 13996-14004.
52. Fabregat, R.; Fabrizio, A.; Meyer, B.; Hollas, D.; Corminboeuf, C., Hamiltonian-Reservoir Replica Exchange and Machine Learning Potentials for Computational Organic Chemistry. *Journal of Chemical Theory and Computation* **2020,** *16* (5), 3084-3094.

TOC

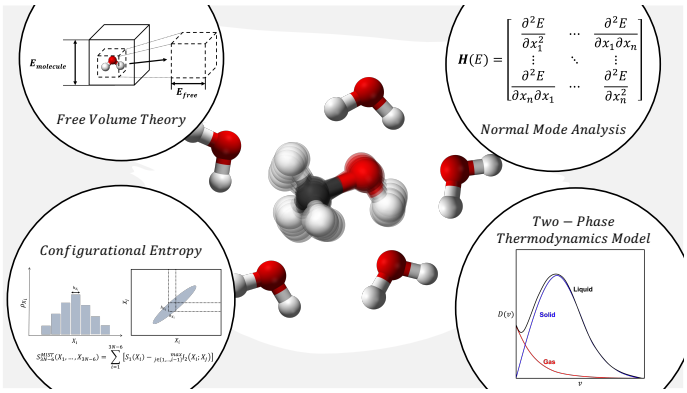
$E_{molecule}$
E_{free}
Free Volume Theory
$H(E) = \begin{bmatrix} \frac{\partial^2 E}{\partial x_1^2} & \cdots & \frac{\partial^2 E}{\partial x_1 \partial x_n} \\ \vdots & \ddots & \vdots \\ \frac{\partial^2 E}{\partial x_n \partial x_1} & \cdots & \frac{\partial^2 E}{\partial x_n^2} \end{bmatrix}$
Normal Mode Analysis
Configurational Entropy
Two − Phase Thermodynamics Model
Liquid
Solid
Gas
$D(v)$
v